Nonlinear Optical Responses of Ternary 2D GeSeTe Nanosheets in NIR Regime

Sumaiya Umme Hani[ab], Safayet Ahmed[ab], Tawsif Ibne Alam[ab], Yuen Hong Tsang[*ab]
[a] Department of Applied Physics, Materials Research Center, and Photonics Research Institute, The Hong Kong Polytechnic University, Hung Hom, Kowloon, Hong Kong, China; [b] Shenzhen Research Institute, The Hong Kong Polytechnic University, Shenzhen 518057, China.

ABSTRACT

Ternary 2D materials, potential candidates for next generation technology showcase boundless opportunities by providing greater degree of freedom through integration of various elements with compositional variety. GeSeTe is a chalcogenide compound with great environmental stability and phase changing feature, making it eligible for many advanced photonics and optoelectronics devices such as ultrafast optical switching, optical modulator, parametric amplifier to name some. In this work, Ternary 2D GeSeTe nanosheets were synthesized employing facile LPE method, followed by extensive characterization have been conducted to comprehend various features of the prepared nanosheets such as thickness, optical absorption etc. Then, the NLO responses of the prepared nanosheets under NIR regime have been realized employing Z-scan methods. The obtained nonlinear absorption coefficient varies from -73 ~ -4.5 cm/GW and -220 ~ -35 cm/GW at 1062 nm and 1560 nm wavelengths respectively indicating superior SA characteristics of GeSeTe nanosheets. The sample nanosheets switched its nonlinear absorption from SA to RSA with increased input intensity enabling potential opportunities for GeSeTe in optical limiting devices. Furthermore, the nonlinear refraction n_2 was recorded to be -9.5×10^{-4} cm^2/GW and -5×10^{-4} cm^2/GW at 1062 nm and 1560 nm respectively. To authors best knowledge, it is the very first time the NLO responses of GeSeTe nanosheets have been investigated and the achieved responses confirms the superior NLO features of GeSeTe that could be widely utilized in various photonics and optoelectronics devices.

Keywords: 2D materials, Ternary, NLO response, Z-scan, OA, CA, Nonlinear absorption, Nonlinear refraction.

1. INTRODUCTION

The exceptional physical, electrical, mechanical, and optical features of low-dimensional layered materials, bearing thickness-dependent bandgaps, great mechanical strength, speedy carrier mobility, firm nonlinear optical properties and good environmental stability have garnered significant interest [1-8]. These low-dimensional materials can be easily transformed into ultrathin nanosheets with unique characteristics and thereby various applications can be probed owing to their weak interlayer interaction. The progression of modern society firmly depends on material, energy and information. The growth of modern society relies on new materials that act as the fundamental source of energy and information. In this cutting-edge era, the technological advancement and the sustainable development have exerted great emphasis on the exploration of novel functional materials and signifies the requirements to investigate their dynamic properties that would challenge the traditional paradigm [9]. Owing to their novel, remarkable and special features, 2D materials offer massive potential in a variety of fields like electronics, spintronics, energy conversion and storage, optoelectronics, and photonics [10-13].

Nonlinear Optics is one intriguing section of photonics and optoelectronics. When materials interact with an electric field of the order of interatomic fields (105–108 V/m) [14, 15], they can display nonlinear optical (NLO) responses. The intriguing nonlinear optical responses, high charge carrier mobility and ultrafast response of these 2D materials have been effectively utilized in wavelength converters, optical limiters, saturable absorbers (SAs) for Q-switching and passive mode locking, and all-optical modulators [16-19]. Over a wide spectral range, graphene showcases nonlinear optical absorption that firmly depends on the input intensity [20-22]. It displays saturable absorption behavior at low pump intensity and transitions to an optical limiting response at higher intensity. It has been discovered that by changing the input intensity, nonlinear absorption can be transitioned from saturable absorption to optical limiting owing to the gapless bandgap

*E-mail: yuen.tsang@polyu.edu.hk , +852-62701374

2D Photonic Materials and Devices VII, edited by Arka Majumdar, Carlos M. Torres, Hui Deng,
Proc. of SPIE Vol. 12888, 1288809 · © 2024 SPIE
0277-786X · doi: 10.1117/12.3015104

structure of graphene [20-21, 23-26]. Nonlinear optical response is a distinctive and dynamic property of 2D materials that can be observed in various other 2D materials beyond graphene, such as BP, Topological insulators (TIs), h-BN, TMCs, perovskites, and their hybrid structures [27-34]. Interestingly, each 2D material has their own distinctive nonlinear optical responses and thereby can be applied to certain advanced photonic and optoelectronics applications [35].

Ternary 2D materials are a significant addition to the 2D platform, combining three distinct elements with varying compositions to produce a variety of unique features. Ternary 2D materials exhibit more dynamic and unique electrical and optical properties than elemental and binary 2D materials because they offer greater flexibility by enabling the combination of different elements in a variety of combinations [36]. To date, a great deal of research has been done on layered ternary materials, focusing on their unique characteristics and electronic structure. Additionally, it is important to highlight that bandgap modification plays a major role in obtaining nonlinear optical properties in 2D materials. Because ternary compounds are made up of three distinct element types with distinct bandgaps, they can effectively change their bandgap distribution [37-39]. Thus, large number of 2D ternary materials can be constructed and with thorough investigation of their various properties they can be employed in various applications. A ternary chalcogenide compound, GeSeTe exhibits several intriguing characteristics, including low phonon energies, tunable photo-induced properties, and high environmental stability to mention a few. Consequently, GeSeTe can be probed into various applications in a variety of industries, including memories, optoelectronics, electronics, and advanced photonics [40-42]. GeSeTe has great potential in NLO devices, photoelectric detection, and microelectronic devices because of its anisotropic nature and superior optical qualities. GeSeTe, similar to other ternary 2D materials, has a configurable bandgap due to compositional change, which offers a range of unique properties [43-44].

In this work, GeSeTe nanosheets have been synthesized with simple Liquid Phase Exfoliation (LPE) method. Followed by several characterizations of the as prepared nanosheets have been performed to comprehend various features such as thickness, chemical composition, crystallinity, uniformity to name some. Afterwards, the nonlinear optical (NLO) responses of the GeSeTe-IPA solution in NIR (1062 nm & 1560 nm) regime have been investigated by Z-scan technique. Employing OA technique, the nonlinear absorption coefficient (β) has been observed and recorded to be -73 ~ -4.5 cm/GW and -220 ~ -35 cm/GW for 1062nm and 1560nm respectively. Moreover, the sample switched its nonlinear absorption behavior from SA to RSA when the input intensity increased to 208.05 MW/cm^2 and 218.23 Mw/cm^2. This imparts a wider range of opportunities for GeSeTe to be integrated in various NLO devices. Further, the nonlinear refraction (n_2) has been calculated as -9.5×10^{-4} cm^2/GW and -5×10^{-4} cm^2/GW at 1062nm & 1560 nm respectively. Based on the acquired results, it can be inferred that the remarkable nonlinear responses of GeSeTe nanosheets make them highly promising for usage in various advanced photonics applications.

2. MATERIAL CHARACTERIZATION

GeSeTe-nanosheets were prepared from the bulk powder by using the simple and inexpensive liquid phase exfoliation (LPE) process, as shown in figure 1(a). Isopropyl alcohol (IPA) was employed as the solvent to dissolve the bulk GeSeTe powder. Two milligrams of powder were added to each milliliter of IPA to create the combination. The mixture was then ultrasonicated for 25 hours at 40 kHz frequency and 400 W of o/p power. By maintaining water circulation during ultrasonication, a constant temperature of 28 °C was maintained, preventing the powder from oxidizing. For five minutes, the GeSeTe-IPA solution was centrifuged (Zonkia HC-3018) at 6000 rpm to make sure the supernatant mixture contained no unexfoliated bulk materials. To further characterize the material, sample was taken from the supernatant and drop-casted over copper grid and quartz substrates.

Figure 1(b) shows the 3D height profile from the AFM image of the GeSeTe nanosheets in 5μm scale. From the image the nano-feature of the prepared nanosheets can be clearly observed as the height of the nanosheets goes maximum up to around 21 nm. Furthermore, 14 flakes were randomly chosen in AFM measurement and figure 1(c) depicts the height of those 14 flakes ranging from 5.7 nm to 12 nm. This further substantiated the 2D feature of the as prepared nanosheets. In order to realize the NLO response of the nanosheets, it is imperative to have a proper uniformity with fabrication process. The UV–vis-NIR spectrum in figure 1(d) showcases the absorption of the prepared nanosheets covering the wavelength from 750–2000 nm. The outcome shows extensive absorption of GeSeTe nanosheets, which is encouraging for a variety of infrared optoelectronic device applications. The SEM image in figure 1(e) showcases the excellent uniformity of the as prepared nanosheets achieved after adopting the LPE method. Figure 1(f) presents the XRD peaks of the GeSeTe nanosheets indicating the firm crystalline state of the nanosheets. Therefore, it can be inferred that with the utilized fabrication process no harsh impact has been imposed on the material.

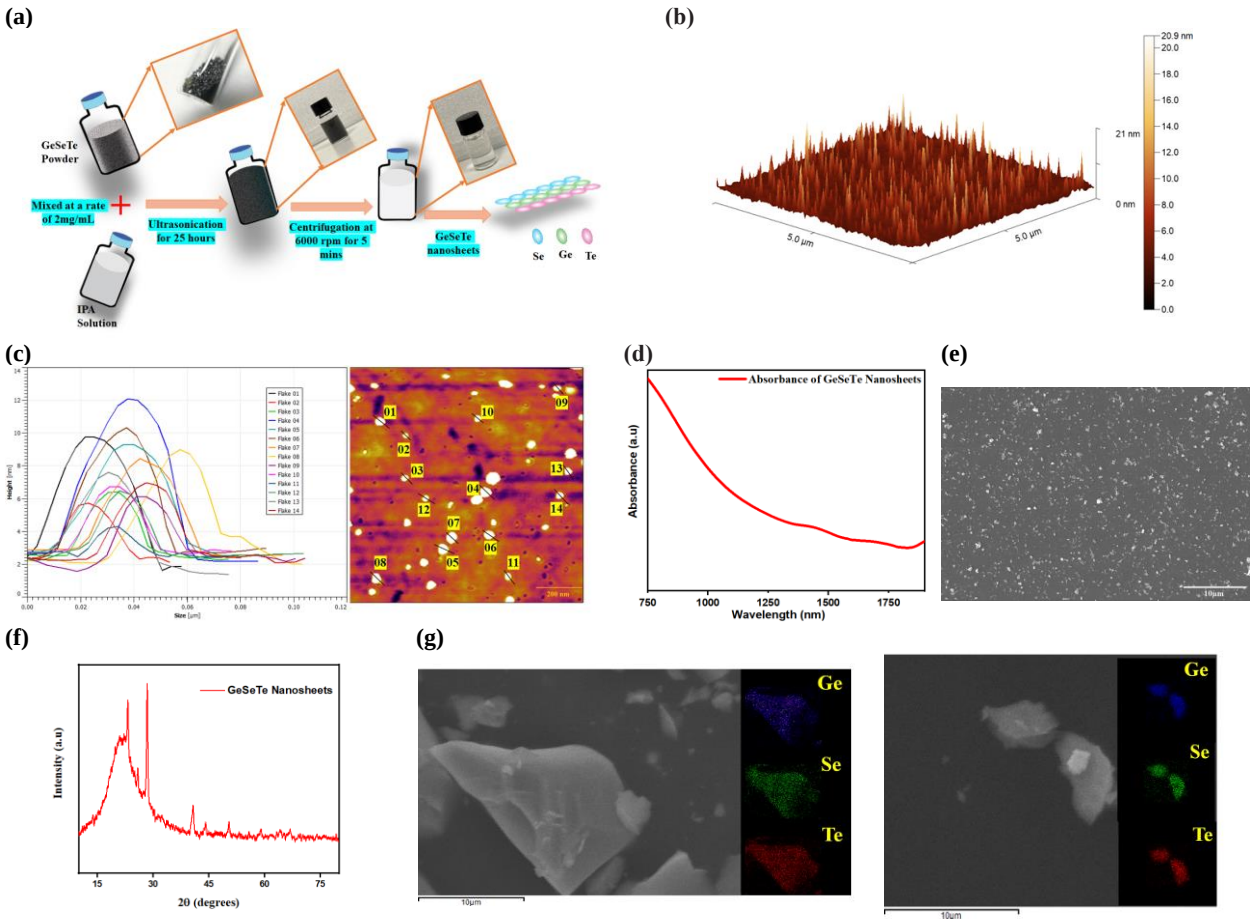

Figure 1: Preparation and Characterization of GeSeTe nanosheets (a) Schematic Diagram of LPE method producing GeSeTe nanosheets, (b) AFM image showing 3D height profile of as prepared Nanosheets in 5µm scale, (c) Height profile of randomly selected 14 flakes, (d) UV-Vis-NIR spectrum of exfoliated nanosheets (e) SEM image of GeSeTe nanosheets, (f) XRD peaks of GeSeTe nanosheets, and (g) distribution of Ge, Se and Te in randomly selected 2 flakes

Finally, these material characterizations allow us to conclude that the prepared samples bear good crystalline state with height profile facilitating 2D feature, great uniformity ensuring no impurity or presence of any other element other than Ge, Se and Te and lastly exhibit broad absorption spectrum.

3. NONLINEAR OPTICAL RESPONSE OF GESETE NANOSHEETS

To date, many experimental methods have been devised to describe the unique nonlinear optical characteristics of photonic materials which include pump-probe (PP) [45], four-wave mixing (FWM) [46], self-phase modulation (SPM) [47], HG [48-50], two-photon-induced fluorescence [51], and Z-scan techniques [52]. All these methods can provide a quantitative understanding of various nonlinear optical features in photonic materials. The fundamental principle behind the simple yet effective experimental method known as Z-scan is the spatial distortion of the transmitted beam at the sample end, including both amplitude and phase distortion. Open aperture (OA) and Closed Aperture (CA) are two common methods of Z-scan technique employed for experimental reasons [53].

In this work, Z-scan was used to observe the broadband NLO responses of the prepared GeSeTe nanosheets using both open aperture (OA) and closed aperture (CA) mechanisms. Two distinct laser systems were used for the Z-scan analysis. Our in-house Mode-locked fiber lasers with 352 fs and 600 fs pulse durations, central wavelengths of 1062 nm and 1560 nm, and having repetition rate of roughly 12.077 MHz and 8.247 MHz were employed as the source laser. The laser beam was focused on Z=0 by a plano-convex lens to ensure a beam waist (w_0) of approximately 58 µm. A drive stage (Thorlabs, DDSM100/M) was used to travel the sample in -z to +z direction. Furthermore, the NLO behavior at 1062 nm and 1560 nm were studied using the two-photodiode power sensors (Thorlabs, S121C and S122C). Figure 2 shows the schematic

diagram of the Z-scan technique. Figure 3 and figure 4 depict the Nonlinear optical responses of GeSeTe-IPA solution at 1062 nm and 1560nm respectively. Figure 3(a-b) and figure 4(a-b) showcase the results obtained from OA methods under 1062 nm and 1560 nm respectively. CA results are given in figure 3(c) and figure 4(c). Lastly, figure 3(d) and figure 4(d) represent the variation of nonlinear absorption coefficient (β) with varying peak intensity of the pump.

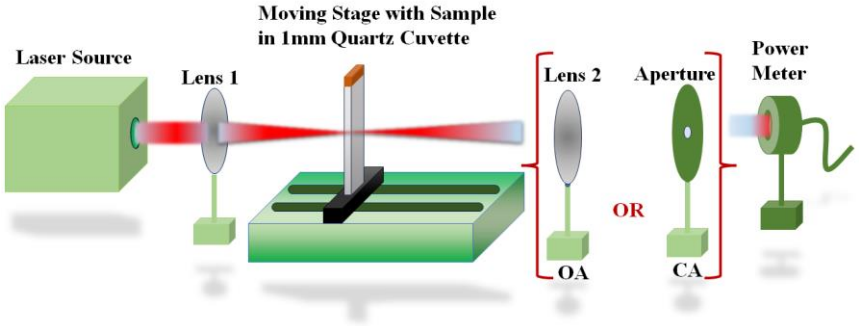

Figure 2: Schematic diagram of Z-scan method where Lens 2 is employed during OA technique and Aperture is used during CA technique

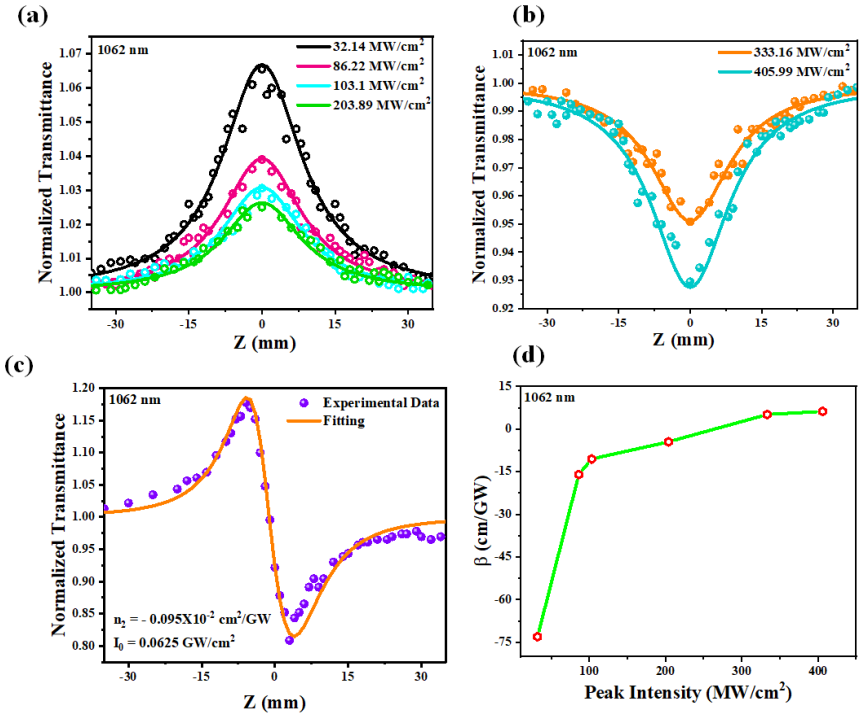

Figure 3: Nonlinear Optical responses of GeSeTe-IPA Sample at 1062 nm (a) OA response of GeSeTe nanosheets under low intensity featuring SA behavior (b) OA response of GeSeTe nanosheets under high intensity featuring RSA behavior (c) CA results (d) Values of β at varying input peak intensity

The nonlinear beam propagation model is used to fit all of the results of the OA method using eq. 1 [53-54] and the nonlinear absorption coefficient (β) was deduced from the fitting results:

$$T(z) = \sum_{n=0}^{\infty} \frac{(-\beta I_0 L_{eff})^n}{\left(1+{z^2}/{z_0^2}\right)^n (n+1)^{3/2}} \approx 1 - \frac{-\beta I_0 L_{eff}}{\left(1+{z^2}/{z_0^2}\right)2^{3/2}} \quad (1)$$

where T(z) is the normalized transmittance, I_0 is the peak intensity at the focus, z_0 is the Rayleigh length, z is the position of the sample, and L_{eff} is the effective length.

From the OA analysis under 1062nm and 1560 nm in figure 3(a) and figure 4(a), it is worth mentioning that with low laser intensities [32.14~203.89MW/cm^2 (1062nm) and 28.91~140.28MW/cm^2 (1560nm)], when the sample goes from -Z to +Z,

the transmittance upsurges, and peaks at Z = 0. Since SA is accountable for these phenomena, in these circumstances the β value is negative [-0.073×10^3~-0.0045×10^{3}cm/GW (1062nm) and -0.220×10^3~0.035×10^{3}cm/GW (1560nm)]. The SA feature can be delineated with Pauli Blocking Principle which forbids the occupancy of electrons at the identical energy level. As the conduction energy level gets occupied with the excited electrons from the valance band, the increasing number of absorbed photons gets saturated and consequently reducing the photon absorption rate and increasing the transmittance [55]. However, with increasing laser intensity (333.16~405.99 MW/cm^2 for 1062nm and 208.05~218.23 MW/cm^2 for 1560nm), the transmittance gradually falls as it approaches the focus point [refer to figure 3(b) and figure 4(b)]. This phenomenon, which is pertinent to the TPA process, is known as RSA. [56]. For the RSA behavior, the recorded β value is positive [0.0051×10^3 ~0.0062×10^{3}cm/GW (1062nm) and 0.075×10^3~0.082×10^3 cm/GW (1560nm)], and with β > 0; as the optical intensity rises, the absorption coefficient gets better, suggesting a decrease in the sample's optical transmission. Usually, the excited-state absorption mechanism is accountable for the change from SA to RSA [53]. Furthermore, the values of imaginary part of third order nonlinear susceptibility [Im ($\chi^{(3)}$)] and FOM (Figure of Merit) were calculated with the help of β and shown in Table 1.

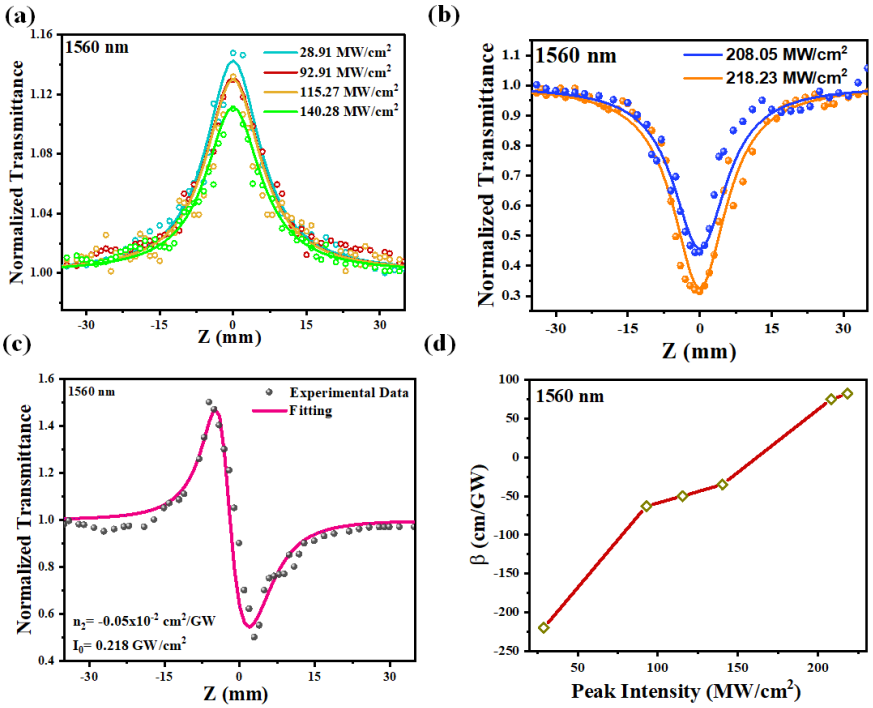

Figure 4: Nonlinear Optical responses of GeSeTe-IPA Sample at 1560 nm (a) OA response of GeSeTe nanosheets under low intensity featuring SA behavior (b) OA response of GeSeTe nanosheets under high intensity featuring RSA behavior (c) CA results (d) Values of β at varying input peak intensity.

The CA Z-scan experimental results under 1062nm and 1560nm were fitted using the following eq. 3, where ΔΦ represents the nonlinear phase shift value [57]. From eq 4, the value of ΔΦ can be calculated, where λ_c is the central wavelength, n_2 is the nonlinear refractive index, L_{eff} is the effective length, and I_0 is the peak intensity at the focus. Moreover, by calculating the values of n_2 from the CA/OA Z-scan findings, the nonlinear refraction response without the nonlinear absorption effect was ascertained [58]. The values of n_2 of the GeSeTe sample were recorded to be -9.5 × 10^{-4} cm^2/GW and -5 × 10^{-4} cm^2/GW at 1062 nm and 1560 nm, respectively.

$$T(z) = \frac{1}{1-\frac{4z/z_0}{\left(1+z^2/z_0^2\right)^2}\Delta\phi+\frac{4}{\left(1+z^2/z_0^2\right)^3}\Delta\phi^2} \quad (2)$$

$$\Delta\phi = \frac{2\pi n_2 I_0 L_{eff}}{\lambda_c} \quad (3)$$

Where, $\Delta\phi$ represents nonlinear phase shift calculated with eq. (3), n_2 is the nonlinear refractive index and λ_c is the central wavelength.

Table 1. Nonlinear Optical parameters obtained from GeSeTe nanosheets in two different wavelengths (1062 nm & 1560 nm) employing OA z-scan method. SA: saturable absorption, RSA: Reverse Saturable absorption and Im $\chi^{3:}$ Imaginary part of third order nonlinear optical susceptibility.

Wavelength, λ [nm]	Nonlinear absorption coefficient, β [cm/GW]	Im χ^3 [$\times 10^{-9}$ esu]	Figure of Merit, FOM [$\times 10^{-9}$ esu cm^{-1}]
1062	-73 [SA]	-0.0467	-0.0101
	-16 [SA]	-0.0102	-0.0023
	-10.5 [SA]	-0.0067	-0.0015
	-4.5 [SA]	-0.0029	-0.00067
	5.1 [RSA]	0.0033	0.00076
	6.2 [RSA]	0.0040	0.00093
1560	-220 [SA]	-0.2070	-0.0210
	-63 [SA]	-0.0593	-0.0061
	-50 [SA]	-0.0471	-0.0048
	-35 [SA]	-0.033	-0.0034
	75 [RSA]	0.0706	0.2651
	82 [RSA]	0.0772	0.0439

The NLO response is known to be highly wavelength dependent [59–60]. This work determines the NLO responses of the GeSeTe nanoparticles at two distinct wavelengths, 1062 nm and 1560 nm, respectively. All the obtained results highlight the great potential of GeSeTe nanomaterials in the field of nonlinear optics.

4. CONCLUSION

In this work nonlinear optical responses, namely nonlinear optical absorption, and nonlinear refraction of 2D ternary GeSeTe nanosheets have been studied employing OA and CA z-scan under two different wavelengths. The admirable values of nonlinear absorption coefficient (β) ranging from -0.073×10^3 ~ -0.0045×10^3cm/GW (for 1062nm) and -0.220×10^3 ~ -0.035×10^3cm/GW (for 1560 nm) depict the superior SA characteristics of the sample material which allows GeSeTe to be effectively employed as SA in ultrafast and ultrashort photonics. Further, with the increase of laser intensity the nonlinear absorption switches its behavior from SA to RSA. Thus, widening the opportunities for GeSeTe to be utilized as optical limiting sensors and devices. Additionally, the large values of third order nonlinear susceptibility [$\chi^{(3)}$], -46×10^{-12} esu (for 1062nm) and -207×10^{-12} esu further substantiate the potential of GeSeTe to be used in ultrafast laser systems. The nonlinear refraction (n_2) was calculated as -9.5×10^{-4} cm^2/GW and -5×10^{-4} cm^2/GW at 1062 nm and 1560 nm, respectively from CA z-scan method. The admirable outcomes indicate the competency of GeSeTe as NLO material and thereby enabling greater prospects of GeSeTe in various advanced photonics and optoelectronics applications.

REFERENCES

[1] Zhang, M., Chen, H., Wang, J., Wang, Z., Zhang, J., Li, J., He, T., Yin, J., Yan, P., & Ruan, S. (2020). Few-layer metal monochalcogenide saturable absorbers for high-energy Q-switched pulse generation. *Nanotechnology*, *31*(20). https://doi.org/10.1088/1361-6528/ab7251

[2] Sun, Z., Martinez, A., & Wang, F. (n.d.). *Optical modulators with two-dimensional layered materials*.

[3] Sargent, E. H. (2012). Colloidal quantum dot solar cells. In *Nature Photonics* (Vol. 6, Issue 3, pp. 133–135). https://doi.org/10.1038/nphoton.2012.33

[4] Martel, R., Schmidt, T., Shea, H. R., Hertel, T., & Avouris, P. (1998). Single-and multi-wall carbon nanotube field-effect transistors. In *APPLIED PHYSICS LETTERS* (Vol. 73). http://apl.aip.org/apl/copyright.jsp

[5] Duan X, Huang Y, Cui Y, Wang J and Lieber C M 2001 Indium phosphide nanowires as building blocks for nanoscale electronic and optoelectronic devices Nature 409 66–9

[6] Comini, E., Faglia, G., Sberveglieri, G., Pan, Z., & Wang, Z. L. (2002). Stable and highly sensitive gas sensors based on semiconducting oxide nanobelts. *Applied Physics Letters*, *81*(10), 1869–1871. https://doi.org/10.1063/1.1504867
[7] Zhou, K. G., Zhao, M., Chang, M. J., Wang, Q., Wu, X. Z., Song, Y., & Zhang, H. L. (2015). Size-dependent nonlinear optical properties of atomically thin transition metal dichalcogenide nanosheets. Small, 11(6), 694–701. https://doi.org/10.1002/smll.201400541
[8] Autere, A., Jussila, H., Dai, Y., Wang, Y., Lipsanen, H., & Sun, Z. (2018). Nonlinear Optics with 2D Layered Materials. In Advanced Materials (Vol. 30, Issue 24). Wiley-VCH Verlag. https://doi.org/10.1002/adma.201705963
[9] Peng, J., Chen, Z., Ding, B., & Cheng, H.-M. (2023b). Recent Advances for the Synthesis and Applications of 2-Dimensional Ternary Layered Materials. Research, 6. https://doi.org/10.34133/research.0040
[10] Xi, X., Wang, Z., Zhao, W., Park, J. H., Law, K. T., Berger, H., Forró, L., Shan, J., & Mak, K. F. (2016). Ising pairing in superconducting NbSe2 atomic layers. Nature Physics, 12(2), 139–143. https://doi.org/10.1038/nphys3538
[11] Splendiani, A., Sun, L., Zhang, Y., Li, T., Kim, J., Chim, C. Y., Galli, G., & Wang, F. (2010). Emerging photoluminescence in monolayer MoS2. Nano Letters, 10(4), 1271–1275. https://doi.org/10.1021/nl903868w
[12] Mudd, G. W., Molas, M. R., Chen, X., Zólyomi, V., Nogajewski, K., Kudrynskyi, Z. R., Kovalyuk, Z. D., Yusa, G., Makarovsky, O., Eaves, L., Potemski, M., Fal'Ko, V. I., & Patanè, A. (2016). The direct-to-indirect band gap crossover in two-dimensional van der Waals Indium Selenide crystals. Scientific Reports, 6. https://doi.org/10.1038/srep39619
[13] Lemme, M. C., Wagner, S., Lee, K., Fan, X., Verbiest, G. J., Wittmann, S., Lukas, S., Dolleman, R. J., Niklaus, F., van der Zant, H. S. J., Duesberg, G. S., & Steeneken, P. G. (2020). Nanoelectromechanical Sensors Based on Suspended 2D Materials. Research, 2020. https://doi.org/10.34133/2020/8748602
[14] You, J. W., Bongu, S. R., Bao, Q., & Panoiu, N. C. (2018). Nonlinear optical properties and applications of 2D materials: Theoretical and experimental aspects. In Nanophotonics (Vol. 8, Issue 1, pp. 63–97). De Gruyter. https://doi.org/10.1515/nanoph-2018-0106
[15] Saleh BEA, Teich MC. Fundamentals of Photonics. New York, Wiley, 1991
[16] Feng, M., Zhan, H., & Chen, Y. (2010). Nonlinear optical and optical limiting properties of graphene families. Applied Physics Letters, 96(3). https://doi.org/10.1063/1.3279148
[17] Wang, G., Marie, X., Gerber, I. C., Amand, T., Lagarde, D., Bouet, L., Vidal, M., Balocchi, A., & Urbaszek, B. (2015). Giant Enhancement of the Optical Second-Harmonic Emission of WSe 2 Monolayers by Laser Excitation at Exciton Resonances Giant Enhance-ment of the Optical Second-Harmonic Emission of WSe 2 Monolayers by Laser Excitation at Exciton. Resonances. Physical Review Letters, 114(9), 10. https://doi.org/10.1103/physrevlett.114.097403ï
[18] Wei, C., Luo, H., Zhang, H., Li, C., Xie, J., Li, J., & Liu, Y. (2016). Passively Q-switched mid-infrared fluoride fiber laser around 3 μm using a tungsten disulfide (WS2) saturable absorber. Laser Physics Letters, 13(10). https://doi.org/10.1088/1612-2011/13/10/105108
[19] Wang, Y., Li, J., Han, L., Lu, R., Hu, Y., Li, Z., & Liu, Y. (2016). Q-switched Tm3+-doped fiber laser with a micro-fiber based black phosphorus saturable absorber. Laser Physics, 26(6). https://doi.org/10.1088/1054-660X/26/6/065104
[20] Bongu, S. R., Bisht, P. B., Namboodiri, R. C. K., Nayak, P., Ramaprabhu, S., Kelly, T. J., Fallon, C., & Costello, J. T. (2014). Influence of localized surface plasmons on Pauli blocking and optical limiting in graphene under femtosecond pumping. Journal of Applied Physics, 116(7). https://doi.org/10.1063/1.4893547
[21] Kalanoor, B. S., Bisht, P. B., Ali, S. A., Baby, T. T., & Ramaprabhu, S. (2012). Optical nonlinearity of silver-decorated graphene.
[22] Demetriou, G., Bookey, H. T., Biancalana, F., Abraham, E., Wang, Y., Ji, W., & Kar, A. K. (2016). Nonlinear optical properties of multilayer graphene in the infrared. Optics Express, 24(12), 13033. https://doi.org/10.1364/oe.24.013033
[23] Ren, J., Zheng, X., Tian, Z., Li, D., Wang, P., & Jia, B. (2016). Giant third-order nonlinearity from low-loss electrochemical graphene oxide film with a high-power stability. Applied Physics Letters, 109(22). https://doi.org/10.1063/1.4969068
[24] Liu, Z., Wang, Y., Zhang, X., Xu, Y., Chen, Y., & Tian, J. (2009). Nonlinear optical properties of graphene oxide in nanosecond and picosecond regimes. Applied Physics Letters, 94(2). https://doi.org/10.1063/1.3068498

[25] Husaini, S., Slagle, J. E., Murray, J. M., Guha, S., Gonzalez, L. P., & Bedford, R. G. (2013). Broadband saturable absorption and optical limiting in graphene-polymer composites. Applied Physics Letters, 102(19). https://doi.org/10.1063/1.4805060
[26] Zhang, X. L., Zhao, X., Liu, Z. B., Shi, S., Zhou, W. Y., Tian, J. G., Xu, Y. F., & Chen, Y. S. (2011). Nonlinear optical and optical limiting properties of graphene oxide-Fe 3O4 hybrid material. Journal of Optics, 13(7). https://doi.org/10.1088/2040-8978/13/7/075202
[27] Varma, S. J., Kumar, J., Liu, Y., Layne, K., Wu, J., Liang, C., Nakanishi, Y., Aliyan, A., Yang, W., Ajayan, P. M., & Thomas, J. (2017). 2D TiS2 Layers: A Superior Nonlinear Optical Limiting Material. Advanced Optical Materials, 5(24). https://doi.org/10.1002/adom.201700713
[28] Xie, Y., Fan, J., Liu, C., Chi, S., Wang, Z., Yu, H., Zhang, H., Mai, Y., & Wang, J. (2018). Giant Two-Photon Absorption in Mixed Halide Perovskite CH3NH3Pb0.75Sn0.25I3 Thin Films and Application to Photodetection at Optical Communication Wavelengths. Advanced Optical Materials, 6(3). https://doi.org/10.1002/adom.201700819
[29] Lu, S., Zhao, C., Zou, Y., Chen, S., Chen, Y., Li, Y., Zhang, H., Wen, S., Tang, D., Stegeman, G. I., Wright, E. M., Finlayson, N., Zanoni, R., & Seaton, C. T. (2013). Nonlinear optical materials; (160.4236) Nanomaterials; (190.3270) Kerr effect; (190.7110) Ultrafast nonlinear optics.
[30] Zheng, Z., Zhao, C., Lu, S., Chen, Y., Li, Y., Zhang, H., Wen, S., Liu, M., Yin, X., Ulin-Avila, E., Geng, B., Zentgraf, T., Ju, L., Wang, F., Zhang, X., Bao, Q., Zhang, H., Wang, B., Ni, Z., … Li, L. J. (2006). Saturated optical absorption through band filling in semiconductors. In Materials: Nanomaterials. References and links (Vol. 1, Issue 16). W.
[31] Yang Xue, Y. X., Zhenda Xie, Z. X., Zhilin Ye, Z. Y., Xiaopeng Hu, X. H., Jinlong Xu, J. X., & Han Zhang, H. Z. (2018). Enhanced saturable absorption of MoS2 black phosphorus composite in 2 μm passively Q-switched Tm: YAP laser. Chinese Optics Letters, 16(2), 020018. https://doi.org/10.3788/col201816.020018
[32] Zhao, G., Zhang, F., Wu, Y., Hao, X., Wang, Z., & Xu, X. (2016). One-Step Exfoliation and Hydroxylation of Boron Nitride Nanosheets with Enhanced Optical Limiting Performance. Advanced Optical Materials, 4(1), 141–146. https://doi.org/10.1002/adom.201500415
[33] Wang, K., Wang, J., Fan, J., Lotya, M., O'Neill, A., Fox, D., Feng, Y., Zhang, X., Jiang, B., Zhao, Q., Zhang, H., Coleman, J. N., Zhang, L., & Blau, W. J. (2013). Ultrafast saturable absorption of two-dimensional MoS2 nanosheets. ACS Nano, 7(10), 9260–9267. https://doi.org/10.1021/nn403886t
[34] Li, D., Jussila, H., Karvonen, L., Ye, G., Lipsanen, H., Chen, X., & Sun, Z. (2015). Polarization and thickness dependent absorption properties of black phosphorus: New saturable absorber for ultrafast pulse generation. Scientific Reports, 5. https://doi.org/10.1038/srep15899
[35] Bykov, A. Y., Murzina, T. V., Rybin, M. G., & Obraztsova, E. D. (2012). Second harmonic generation in multilayer graphene induced by direct electric current. https://doi.org/10.1103/PhysRevB.85.121413
[36] Peng, J., Chen, Z., Ding, B., & Cheng, H.-M. (2023b). Recent Advances for the Synthesis and Applications of 2-Dimensional Ternary Layered Materials. Research, 6. https://doi.org/10.34133/research.0040
[37] Wei, B. N., Jiao, Z. H., & Liu, W. J. (2021). Ternary transition metal dichalcogenides for passively Q-switched Er-doped fiber laser applications. Optik, 248. https://doi.org/10.1016/j.ijleo.2021.168096
[38] Liu, W., Liu, M., Liu, X., Lei, M., & Wei, Z. (2020). SnSSe as a saturable absorber for an ultrafast laser with superior stability. Optics Letters, 45(2), 419. https://doi.org/10.1364/ol.380183
[39] Li, L., Pang, L., Wang, Y., & Liu, W. (2021). $W_XNb_{(1-x)}Se_2$ nanosheets for ultrafast photonics. Nanoscale, 13(4), 2511–2518. https://doi.org/10.1039/d0nr08580d
[40] Cheruvalath, A., Sebastian, I., Sebastian, M., Nampoori, V. P. N., & Thomas, S. (2017). Effect of midgap defect states on the optical properties of Ge20Se70Te10 nano colloids. Optical Materials, 72, 265–269. https://doi.org/10.1016/j.optmat.2017.06.010
[41] Černošek, Z., Černošková, E., Hejdová, M., Holubová, J., & Todorov, R. (2017). The properties and structure of Ge-Se-Te glasses and thin films. Journal of Non-Crystalline Solids, 460, 169–177. https://doi.org/10.1016/j.jnoncrysol.2017.01.032
[42] Sharma, P., & Katyal, S. C. (2009). Effect of substrate temperature on the optical parameters of thermally evaporated Ge-Se-Te thin films. Thin Solid Films, 517(13), 3813–3816. https://doi.org/10.1016/j.tsf.2009.01.106
[43] Sharma, P., & Katyal, S. C. (2007). Thickness dependence of optical parameters for Ge-Se-Te thin films. Materials Letters, 61(23–24), 4516–4518. https://doi.org/10.1016/j.matlet.2007.02.040

[44] Sharma, P., & Katyal, S. C. (2008). Effect of deposition parameters on the optical energy gap and refractive index of a-Ge-Se-Te thin films. Philosophical Magazine, 88(17), 2549–2557. https://doi.org/10.1080/14786430802375675
[45] Olsen, T., Jacobsen, K. W., & Thygesen, K. S. (2011). Large Excitonic Effects in the Optical Properties of Monolayer MoS2. http://arxiv.org/abs/1107.0600
[46] Hendry, E., Hale, P. J., Moger, J. J., Savchenko, A. K., & Mikhailov, S. A. (2009). Strong nonlinear optical response of graphene flakes measured by four-wave mixing. https://doi.org/10.1103/PhysRevLett.105.097401
[47] Wu, R., Zhang, Y., Yan, S., Bian, F., Wang, W., Bai, X., Lu, X., Zhao, J., & Wang, E. (2011). Purely coherent nonlinear optical response in solution dispersions of graphene sheets. Nano Letters, 11(12), 5159–5164. https://doi.org/10.1021/nl2023405
[48] Säynätjoki, A., Karvonen, L., Riikonen, J., Kim, W., Mehravar, S., Norwood, R. A., Peyghambarian, N., Lipsanen, H., & Kieu, K. (2013). Rapid large-area multiphoton microscopy for characterization of graphene. ACS Nano, 7(10), 8441–8446. https://doi.org/10.1021/nn4042909
[49] Autere, A., Ryder, C. R., Säynätjoki, A., Karvonen, L., Amirsolaimani, B., Norwood, R. A., Peyghambarian, N., Kieu, K., Lipsanen, H., Hersam, M. C., & Sun, Z. (2017). Rapid and Large-Area Characterization of Exfoliated Black Phosphorus Using Third-Harmonic Generation Microscopy. Journal of Physical Chemistry Letters, 8(7), 1343–1350. https://doi.org/10.1021/acs.jpclett.7b00140
[50] Wang, R., Chien, H. C., Kumar, J., Kumar, N., Chiu, H. Y., & Zhao, H. (2014). Third-harmonic generation in ultrathin films of MoS2. ACS Applied Materials and Interfaces, 6(1), 314–318. https://doi.org/10.1021/am4042542
[51] Kaiser, %, & Garrett, C. G. B. (1961). PHYSICAL REVIEW LETTERS TWO-PHOTON EXCITATION IN CaF Eu'+ (Vol. 7, Issue 6).
[52] De Araújo, C. B., Gomes, A. S. L., & Boudebs, G. (2016). Techniques for nonlinear optical characterization of materials: A review. In Reports on Progress in Physics (Vol. 79, Issue 3). Institute of Physics Publishing. https://doi.org/10.1088/0034-4885/79/3/036401
[53] Ahmed, S., Cheng, P. K., Qiao, J., Gao, W., Saleque, A. M., Al Subri Ivan, M. N., Wang, T., Alam, T. I., Hani, S. U., Guo, Z. L., Yu, S. F., & Tsang, Y. H. (2022). Nonlinear Optical Activities in Two-Dimensional Gallium Sulfide: A Comprehensive Study. ACS Nano, 16(8), 12390–12402. https://doi.org/10.1021/acsnano.2c03566
[54] Xu, N., Li, H., Gan, Y., Chen, H., Li, W., Zhang, F., Jiang, X., Shi, Y., Liu, J., Wen, Q., & Zhang, H. (2020). Zero-Dimensional MXene-Based Optical Devices for Ultrafast and Ultranarrow Photonics Applications. Advanced Science, 7(22). https://doi.org/10.1002/advs.202002209
[55] Ye, C., Yang, Z., Dong, J., Huang, Y., Song, M., Sa, B., Zheng, J., & Zhan, H. (2021). Layer-Tunable Nonlinear Optical Characteristics and Photocarrier Dynamics of 2D PdSe2 in Broadband Spectra. Small, 17(50). https://doi.org/10.1002/smll.202103938
[56] Zaręba, J. K., Nyk, M., & Samoć, M. (2021). Nonlinear Optical Properties of Emerging Nano- and Microcrystalline Materials. In Advanced Optical Materials (Vol. 9, Issue 23). John Wiley and Sons Inc. https://doi.org/10.1002/adom.202100216
[57] Cheng, P. K., Ahmed, S., Qiao, J., Wong, L. W., Yuen, C. F., Saleque, A. M., Ivan, M. N. A. S., Hani, S. U., Hossain, M. I., Zhao, J., Wen, Q., & Tsang, Y. H. (2022). Nonlinear optical properties of two-dimensional palladium ditelluride (PdTe2) and its application as aerosol jet printed saturable absorbers for broadband ultrafast photonics. In Applied Materials Today (Vol. 26). Elsevier Ltd. https://doi.org/10.1016/j.apmt.2021.101296
[58] Lee, J., Lee, K., Kwon, S., Shin, B., & Lee, J. H. (2019). Investigation of nonlinear optical properties of rhenium diselenide and its application as a femtosecond mode-locker. Photonics Research, 7(9), 984. https://doi.org/10.1364/prj.7.000984
[59] He, J., Ji, W., Ma, G. H., Tang, S. H., Elim, H. I., Sun, W. X., Zhang, Z. H., & Chin, W. S. (n.d.). Excitonic nonlinear absorption in CdS nanocrystals studied using Z-scan technique.
[60] Jang, J. I., Park, S., Clark, D. J., Saouma, F. O., Lombardo, D., Harrison, C. M., & Shim, B. (2013). Impact of two-photon absorption on second-harmonic generation in CdTe as probed by wavelength-dependent Z-scan nonlinear spectroscopy. Journal of the Optical Society of America B, 30(8), 2292. https://doi.org/10.1364/josab.30.002292